

Cite this: *Nanoscale Adv.*, 2023, 5, 2873Received 6th February 2023  
Accepted 29th April 2023

DOI: 10.1039/d3na00087g

rsc.li/nanoscale-advances

## Preparation of water-dispersed monolayer LDH nanosheets by SMA intercalation to hinder the restacking upon redispersion in water†

Qingqing Qin,<sup>ab</sup> Yingmo Hu,<sup>ab</sup> Junya Wang,<sup>c</sup> Yuanyuan Yang,<sup>b</sup> Ting Lei,<sup>b</sup> Zhenyu Cui,<sup>d</sup> Sufang Guo<sup>a</sup> and Shuhao Qin<sup>ab</sup>

We present a novel method for preparing water-dispersed monolayer layered double hydroxide (LDH) nanosheets (m-LDH). By intercalating styrene-maleic anhydride copolymer (SMA) into LDH, we obtained m-LDH through a simple aging step that produced stable, translucent colloidal solutions. After drying, the resulting powder can be redispersed in water to recover the m-LDH monolayer structure. To our knowledge, this is the first report of immediate recovery of the m-LDH monolayer structure from dried powder after redispersion in water. Our method may have significant implications for preparing and utilizing m-LDH nanosheets in various applications.

Monolayer two-dimensional (2D) materials such as monolayer graphene,<sup>1,2</sup> MoS<sub>2</sub>,<sup>3</sup> phosphorene,<sup>4</sup> and layered double hydroxides (LDHs)<sup>5,6</sup> have attracted wide attention because these atom-thin 2D materials have anisotropy,<sup>7</sup> with thicknesses of around 1 nm and lateral sizes ranging from submicrons to several tens of microns.<sup>8</sup> These materials have a large applicability spectrum, including electromagnetic wave absorbers,<sup>9,10</sup> sensors,<sup>11–13</sup> environment applications,<sup>14–16</sup> supercapacitors,<sup>17–19</sup> and catalysis.<sup>20–22</sup> LDHs are a class of ionic layered compounds comprising positively charged hydroxide layers sandwiched between charge-balancing anions and water molecules. They have great potential in developing new nanomaterials due to their unique versatility.<sup>23,24</sup> For example, their flexible chemical composition allows the design of various nanomaterials by just

changing the metal cations.<sup>25</sup> Monolayer LDH nanosheets usually exhibit better properties than intercalated nanocomposites, making them highly desirable for synthesis.<sup>26,27</sup>

In recent years, there have been many strategies for synthesizing monolayer LDH nanosheets. These could be mainly divided into bottom-up strategies (reverse microemulsion method,<sup>28,29</sup> layer growth inhibitor method,<sup>27,30</sup> separation–nucleation–aging step method,<sup>7</sup> *etc.*) and top-down strategies (liquid phase exfoliation,<sup>31,32</sup> gas phase exfoliation,<sup>33</sup> plasma treatment,<sup>34</sup> *etc.*). Although these methods can obtain monolayer LDH nanosheets, the preparation process is often too complex, and the synthesis time could be long. In addition, after drying, the monolayer LDH nanosheets easily restack and lose the monolayer structure, and the process is irreversible.<sup>7,35</sup> Therefore, the monolayer LDH nanosheets obtained by these methods are usually wet.<sup>7</sup> However, LDH powder materials are easier to store and transport than wet materials. Wang *et al.* successfully prepared monolayer LDH powder using an aqueous miscible organic solvent treatment. However, the monolayer LDH powder easily loses the monolayer structure in the presence of water.<sup>36</sup> Therefore, it is important to design a simple method for the synthesis of monolayer LDH nanosheets and its powder that can quickly delaminate into monolayer LDH nanosheets in water.

In this contribution, we report a simple method for synthesizing monolayer LDH nanosheets in water using MgAl-LDH. The as-obtained powder can be immediately delaminated into monolayer nanosheets upon redispersion in water. The key was employing a binary carboxylate polymer obtained from the styrene-maleic anhydride copolymer (SMA) ring opening in an alkaline environment as a charge compensation anion during the synthesis of LDH (Scheme 1). This new form of SMA intercalated MgAl-LDH nanocomposite (SMA-LDH) has a large particle size of approximately 2 μm. Moreover, monolayer SMA-LDH nanosheets (m-LDH) with a lateral size of approximately 30 nm were directly obtained after aging.

The resulting dispersed product of SMA-LDH and m-LDH are shown in Fig. S1.† The SMA-LDH aqueous dispersion exhibited

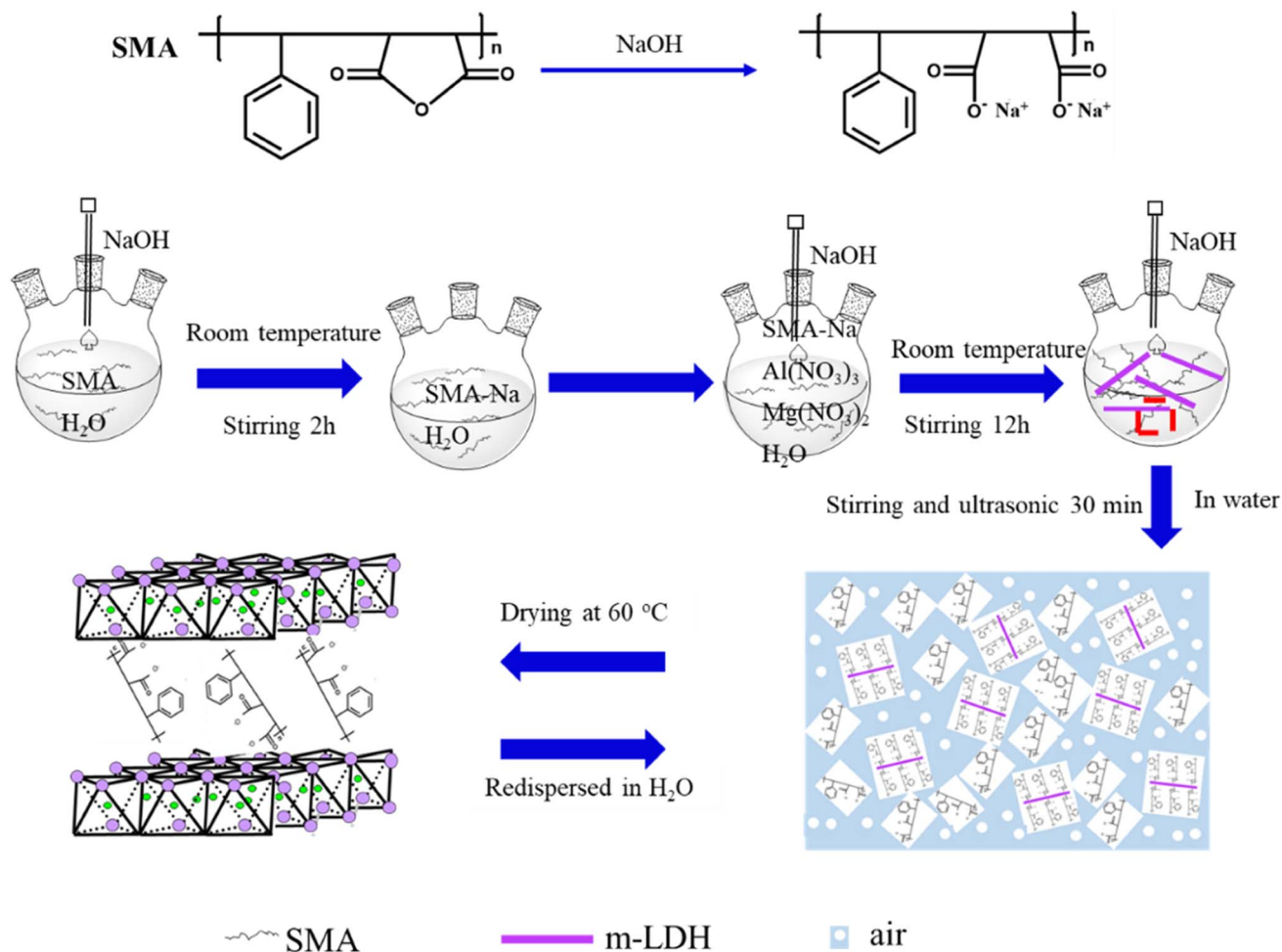
<sup>a</sup>Engineering Research Center of Ministry of Education for Geological Carbon Storage and Low Carbon Utilization of Resources, Beijing Key Laboratory of Materials Utilization of Nonmetallic Minerals and Solid Wastes, National Laboratory of Mineral Materials, School of Material Sciences and Technology, China University of Geosciences, Beijing 100083, China. E-mail: huyingmo@cugb.edu.cn

<sup>b</sup>Guizhou Material Industry Technology Research Institute, Guiyang, 550025, China. E-mail: pec.shqin@gzu.edu.cn

<sup>c</sup>Faculty of Environmental Science and Engineering, Kunming University of Science and Technology, Kunming, 650500, China

<sup>d</sup>School of Materials Science and Engineering, Tiangong University, Tianjin, 300387, PR China

† Electronic supplementary information (ESI) available. See DOI: <https://doi.org/10.1039/d3na00087g>



Scheme 1 The synthesis of water-dispersed m-LDH.

the Tyndall effect (Fig. S1 inset†), supporting the existence of colloidal LDH in the aged mixture.<sup>7</sup> The m-LDH gel was collected by centrifugation and investigated by X-ray diffraction (XRD) when the gel was in an air atmosphere at different times (Fig. 1a). The m-LDH gel did not show any (00 $l$ ) peak, but a (110) peak was observed at *ca.* 60°. These results indicate the presence of monolayer LDH nanosheets without stacking along the *c*-axis and the formation of a 2D crystalline nanosheet structure.<sup>7,20,36</sup> The peak at 20°–50° could be attributed to water in the gel.<sup>7</sup> These results demonstrate that the SMA can inhibit the growth of LDH nanosheets along the *c*-axis, allowing the monolayer LDH nanosheets to grow laterally.

The XRD patterns of the m-LDH gel in an air atmosphere for 60 min showed sharp peaks located at *ca.* 35.4° and 61.5°, but no low diffraction angle peak. After 180 min in an air atmosphere, the gel was almost dry. The sharp peaks located at 5°, 11.7°, 20.6°, 35.4°, and 61.5° can be attributed to the (003), (006), (009), (012) and (110) planes, respectively.<sup>37</sup> Compared with the MgAl-LDH (magnesium aluminium hydroxide, JCPDS22-700), the 003 characteristic peak shifted to lower diffraction degrees. This confirms the formation of the LDH structure and demonstrates that the m-LDH was able to restore

its layer structure after drying, with the interlayer distance being enlarged to 1.78 nm by the SMA.<sup>38</sup> When the m-LDH gel was dried at 60 °C, the XRD peak shape was similar to that of the gel in an air atmosphere for 180 min, indicating that the SMA acted as interlayer gallery anions intercalated in the interlayer space of LDH (Fig. 1b). These results support the successful synthesis of SMA-LDH and water-dispersed m-LDH by the coprecipitation method.

To investigate the relationship between the SMA as an interlayer anion and the positive LDH layer, the elemental compositions of the SMA-LDH were analysed using EDS (Fig. S2†), and the chemical groups of the m-LDH gel, the m-LDH gel in an air atmosphere for 180 min, and the SMA-LDH were characterized by ATR-FTIR, as shown in Fig. 1c. Fig. S2† shows that Mg, Al, C, and O were detected in the powder. Fig. 1c shows strong absorption bands at 3449–3393  $\text{cm}^{-1}$  assigned to OH stretching bands, while the band at *ca.* 1635  $\text{cm}^{-1}$  is due to the water molecule bending vibrations. The bands at around 720  $\text{cm}^{-1}$  are assigned to the metal oxide vibrations.<sup>25,39</sup> The bands located at 2917 and 2871  $\text{cm}^{-1}$  are attributed to the C–H vibrations of the alkyl chain. The bands at *ca.* 1553  $\text{cm}^{-1}$  and 1412  $\text{cm}^{-1}$  are attributed to the  $\text{COO}^-$  functional group



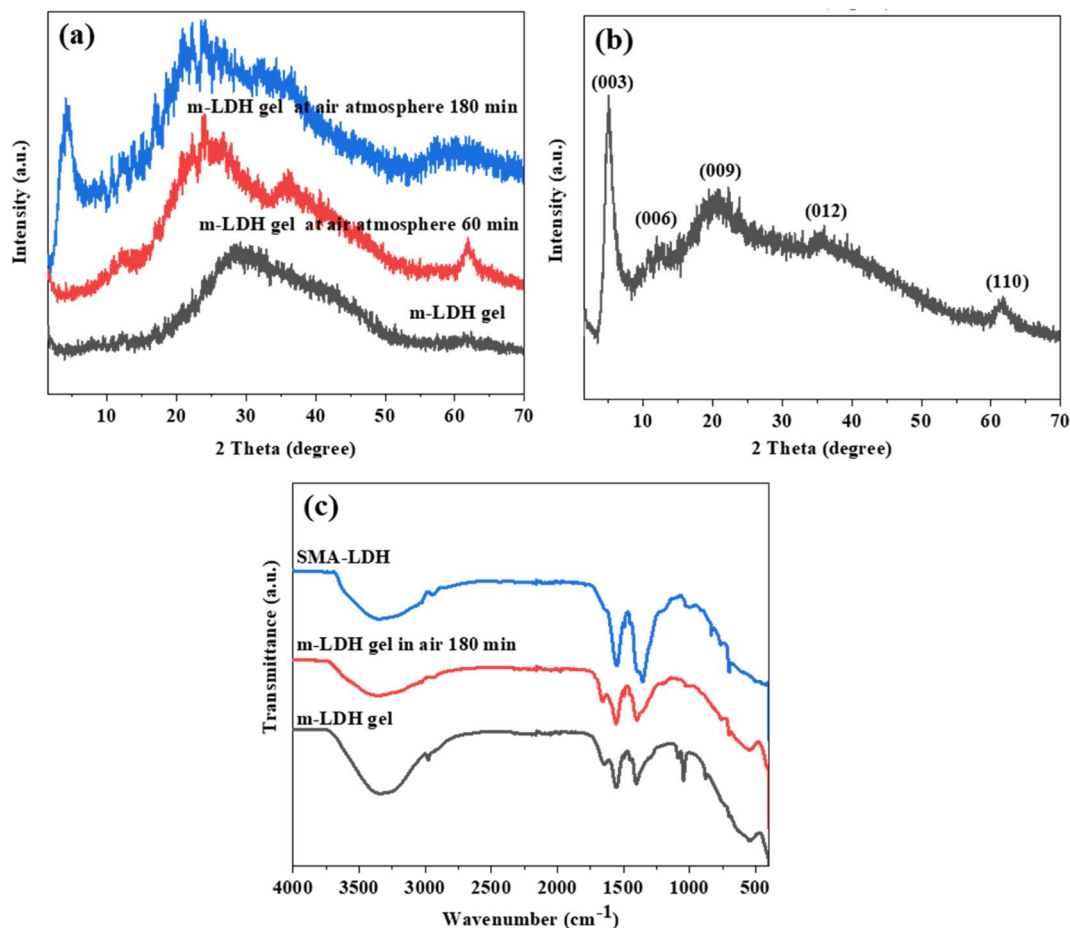


Fig. 1 (a) XRD patterns of m-LDH gel in an air atmosphere for different times, (b) XRD pattern of SMA-LDH (dried at 60 °C), and (c) ATR-FTIR spectra of m-LDH gel, m-LDH gel in air for 180 min and SMA-LDH.

stretching vibrations, and the vibration peaks of C=C in the benzene ring bond are located at 1495 cm<sup>-1</sup> and 1454 cm<sup>-1</sup>. The out-of-plane bending vibration peaks of the single substituted benzene ring C-H bond are located at 1090 cm<sup>-1</sup> and 1045 cm<sup>-1</sup>.<sup>40,41</sup> These results further confirmed the successful synthesis of LDH intercalated with SMA, indicating that the SMA as an interlayer anion readily adheres to the surface of the positive LDH layer.

To further prove the successful synthesis of m-LDH, the m-LDH was characterized by TEM and AFM, and SMA-LDH was characterized by SEM. Fig. 2a shows that the highly dispersed m-LDH has a typical pseudohexagonal morphology with a size distribution of *ca.* 30 nm in diameter, which differs from the SMA-LDH particles' stone-like morphology (Fig. S3†). Fig. 2c and d further confirm the ultrathin structure of m-LDH. The thickness of m-LDH determined *via* this technique was *ca.* 0.8 nm. The theoretical thickness of a single layer of metal hydroxide is *ca.* 0.48 nm.<sup>7,35,36</sup> Possible adsorption of SMA on the nanosheet surface may be responsible for the deviation of ~0.30 nm, or the van der Waals radius of hydrogen atoms (0.12 nm) may account for it.<sup>30,42,43</sup> The lattice fringe spacing of 0.15 nm corresponding to the LDH (110) plane can be observed in Fig. 2b, revealing the successful preparation of the LDH

structure.<sup>20,29</sup> These results support the successful synthesis of water-dispersed m-LDH after aging.

Although monolayer LDH nanosheets have been reported in water,<sup>32</sup> they often restack during separation and drying. Therefore, the monolayer LDH nanosheets cannot be immediately obtained *via* simple procedures.<sup>7,36,44</sup> Our results show that SMA-LDH has high dispersion in water (Fig. 3), and when SMA-LDH is redispersed in water, m-LDH can be obtained immediately (denoted as r-m-LDH). These outcomes indicate that SMA allows the powder to delaminate into monolayer nanosheets in water and obtain water-dispersed m-LDH. Moreover, losing the monolayer structure after drying and regaining it after powder redispersion in water is reversible. This process represents a step-change in LDH chemistry.

During the synthesis of water-dispersed m-LDH, SMA may serve multiple functions. SMA is a highly polar polymer.<sup>40</sup> In an alkaline environment, the ring opening reaction of SMA produces a polymer containing dicarboxylate to form a new surfactant, thus forming a foam solution. On the one hand, the ring opened SMA as an interlayer gallery anion can adhere to the LDH sheet surface, enlarging the interlayer distance to weaken the electrostatic forces among the hydroxide sheets and render the LDH layers hydrophobic. This lowers layer-layer





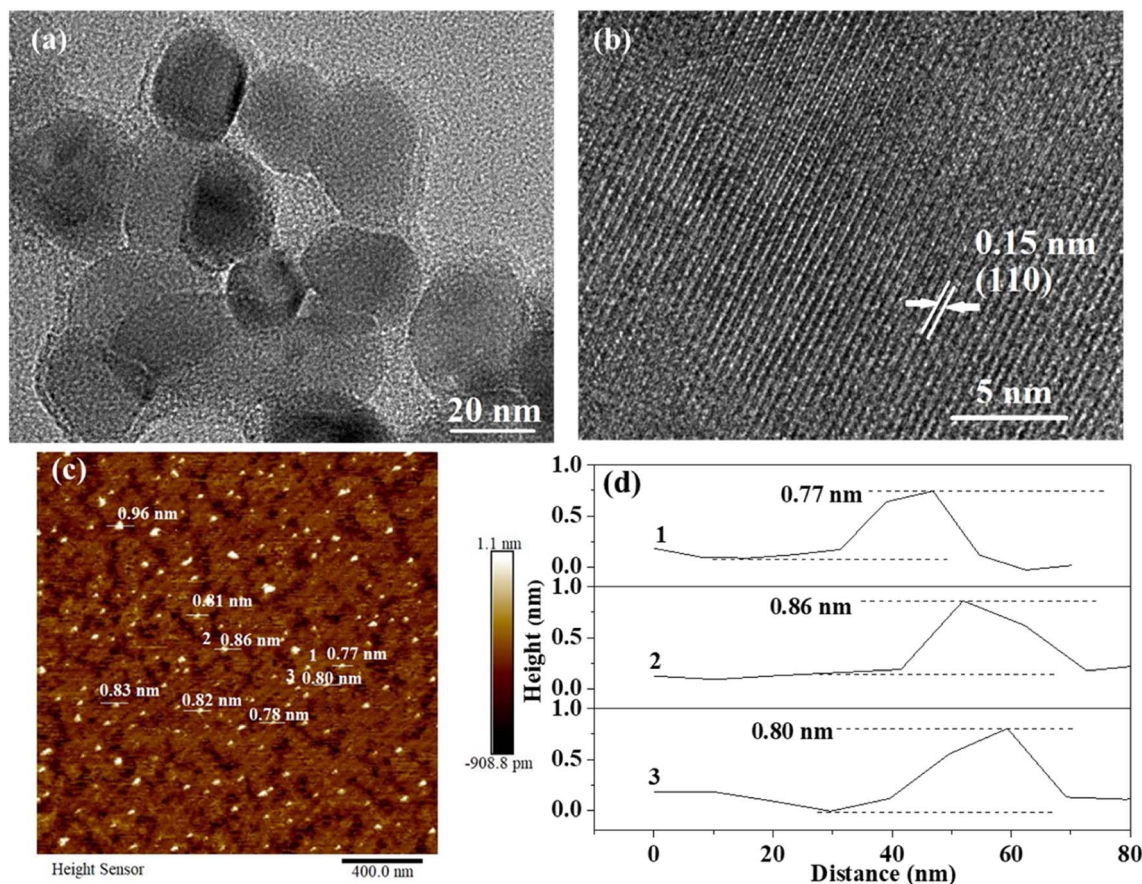


Fig. 2 (a) TEM image of m-LDH, (b) HRTEM image of m-LDH, (c) AFM image of m-LDH, and (d) AFM height profiles of m-LDH, the numbers 1–3 in (c) correspond to the profiles 1–3 in (d).

interactions, preventing layer–layer restacking in water and allowing for the delamination of powder into m-LDH after being dispersed in water.<sup>30,32</sup> On the other hand, due to the foam solution containing a lot of air, the SMA attached to the LDH sheet surface allows air to be positioned in the interlayer of SMA-LDH, further avoiding LDH layer stacking.<sup>45</sup>

For instance, SMA intercalated ZnFe-LDH (SMA-ZnFe-LDH) and its monolayer nanosheets (m-ZnFe LDH) have been prepared through a simple coprecipitation using SMA as interlayer gallery anions and layer growth inhibitor. Moreover, m-ZnFe LDH loses its monolayer structure after drying. The monolayer structure can be immediately recovered (denoted as

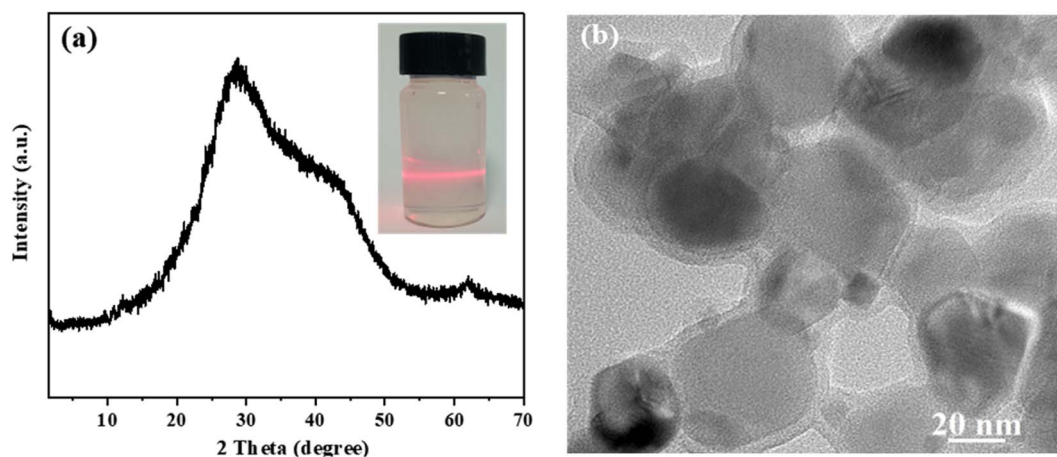


Fig. 3 (a) XRD pattern of r-m-LDH, inset: highly dispersed r-m-LDH with a clear Tyndall effect and (b) TEM image of r-m-LDH.



r-m-ZnFe LDH) after the powder is redispersed in water (see Fig. S4–S6†). Based on the general principles of water-dispersed monolayer LDH preparation (Scheme 1), it is supposed that different types of water-dispersed monolayer LDH nanosheets can be prepared by changing the metal cations.

In conclusion, this study presents a novel method to synthesize water-dispersed monolayer LDH nanosheets using SMA intercalated LDH. Various morpho-structural methods showed that m-LDH can be obtained after aging. The dried m-LDH can delaminate into monolayer nanosheets immediately after the powder is redispersed in water. Moreover, this process of losing the monolayer structure after drying and regaining it after the powder is redispersed in water is reversible. We anticipate that SMA-LDH and its monolayer nanosheets will significantly impact various applications.

## Author contributions

Qingqing Qin: writing – original draft. Yingmo Hu: resources, supervision, writing-review & editing. Junya Wang, Yuanyuan Yang, Ting Lei, Zhenyu Cui, and Sufang Guo: investigation. Shuhao Qin: conceptualization, methodology, resources, supervision, writing-review & editing.

## Conflicts of interest

There are no conflicts to declare.

## Acknowledgements

This work was supported by the Science and Technology Planning Project of Guizhou Province ([2020]4Y021 and [2021]9), the Science and Technology Planning Project of Guiyang ([2020]-18-9 and [2021]-1-1), and the Science and Technology Planning Project of Baiyun district of Guiyang ([2020]30).

## References

- 1 Z. Fan, R. Liu and X. Cheng, *Coatings*, 2021, **11**, 424–437.
- 2 D. Sharma, A. V. Menon and S. Bose, *Nanoscale Adv.*, 2020, **2**, 3292–3303.
- 3 C. Q. Li, X. Shen, R. C. Ding and G. S. Wang, *Chempluschem*, 2019, **84**, 226–232.
- 4 G. Alberti, M. Casciola and U. Costantino, *J. Colloid Interface Sci.*, 1985, **107**, 256–263.
- 5 Q. Wang, J. P. Undrell, Y. Gao, G. Cai, J.-C. Buffet, C. A. Wilkie and D. O'Hare, *Macromolecules*, 2013, **46**, 6145–6150.
- 6 J. Wang, X. Mei, L. Huang, Q. Zheng, Y. Qiao, K. Zang, S. Mao, R. Yang, Z. Zhang, Y. Gao, Z. Guo, Z. Huang and Q. Wang, *J. Energy Chem.*, 2015, **24**, 127–137.
- 7 H. Chi, J. Dong, T. Li, S. Bai, L. Tan, J. Wang, T. Shen, G. Liu, L. Liu, L. Sun, Y. Zhao and Y.-F. Song, *Green Energy Environ.*, 2022, **7**, 975–982.
- 8 S. Werner, V. W. Lau, S. Hug, V. Duppel, H. Clausen-Schaumann and B. V. Lotsch, *Langmuir*, 2013, **29**, 9199–9207.
- 9 X. Gao, Z. Jia, B. Wang, X. Wu, T. Sun, X. Liu, Q. Chi and G. Wu, *Chem. Eng. J.*, 2021, **419**, 130019–130030.
- 10 Z. Wang, L. Yang, Y. Zhou, C. Xu, M. Yan and C. Wu, *ACS Appl. Mater. Interfaces*, 2021, **13**, 16713–16721.
- 11 S. Ippili, V. Jella, A. M. Thomas, C. Yoon, J.-S. Jung and S.-G. Yoon, *J. Mater. Chem. A*, 2021, **9**, 15993–16005.
- 12 Q. Chen, X. Wang, Z. Wang, J. Cao, J. Dai, J. Wang, E. Fatima-Ezzahra and X. Huang, *ACS Appl. Nano Mater.*, 2022, **5**, 4991–4997.
- 13 M. Li, L. Fang, H. Zhou, F. Wu, Y. Lu, H. Luo, Y. Zhang and B. Hu, *Appl. Surf. Sci.*, 2019, **495**, 143554–143562.
- 14 A. A. H. Faisal, Z. K. Ramadhan, N. Al-Ansari, G. Sharma, M. Naushad and C. Bathula, *Chemosphere*, 2022, **291**, 132693–132701.
- 15 A. A. Wani, A. M. Khan, Y. K. Manea, M. A. S. Salem and M. Shahadat, *J. Hazard. Mater.*, 2021, **416**, 125754.
- 16 M. Abbasi, M. M. Sabzehmeidani, M. Ghaedi, R. Jannesar and A. Shokrollahi, *Mater. Sci. Eng., B*, 2021, **267**, 115086–115095.
- 17 N. S. Padalkar, S. V. Sadavar, R. B. Shinde, A. S. Patil, U. M. Patil, D. S. Dhawale, R. N. Bulakhe, H. Kim, H. Im, A. Vinu, C. D. Lokhande and J. L. Gunjekar, *J. Colloid Interface Sci.*, 2022, **616**, 548–559.
- 18 C. Lai, Y. Wang, L. Fu, H. Song, B. Liu, D. Pan, Z. Guo, I. Seok, K. Li, H. Zhang and M. Dong, *Adv. Compos. Hybrid Mater.*, 2021, **5**, 536–546.
- 19 M. M. Baig, M. T. Mehran, R. Khan, K. Mahmood, S. R. Naqvi, A. H. Khoja and I. H. Gul, *Surf. Coat. Technol.*, 2021, **421**, 127445–127455.
- 20 Z. Wang, S. M. Xu, Y. Xu, L. Tan, X. Wang, Y. Zhao, H. Duan and Y. F. Song, *Chem. Sci.*, 2019, **10**, 378–384.
- 21 W. Huo, T. Cao, X. Liu, W. Xu, B. Dong, Y. Zhang and F. Dong, *Green Energy Environ.*, 2019, **4**, 270–277.
- 22 X. Jia, Y. Zhao, G. Chen, L. Shang, R. Shi, X. Kang, G. I. N. Waterhouse, L.-Z. Wu, C.-H. Tung and T. Zhang, *Adv. Energy Mater.*, 2016, **6**, 1502585–1502590.
- 23 B. Liu, Z. Zheng, Y. Liu, M. Zhang, Y. Wang, Y. Wan and K. Yan, *J. Energy Chem.*, 2023, **78**, 412–421.
- 24 M. Zhang, Y. Liu, B. Liu, Z. Chen, H. Xu and K. Yan, *ACS Catal.*, 2020, **10**, 5179–5189.
- 25 Q. Wang, H. H. Tay, D. J. Ng, L. Chen, Y. Liu, J. Chang, Z. Zhong, J. Luo and A. Borgna, *ChemSusChem*, 2010, **3**, 965–973.
- 26 P. Xiong, X. Zhang, H. Wan, S. Wang, Y. Zhao, J. Zhang, D. Zhou, W. Gao, R. Ma, T. Sasaki and G. Wang, *Nano Lett.*, 2019, **19**, 4518–4526.
- 27 L. Tan, S. M. Xu, Z. Wang, Y. Xu, X. Wang, X. Hao, S. Bai, C. Ning, Y. Wang, W. Zhang, Y. K. Jo, S. J. Hwang, X. Cao, X. Zheng, H. Yan, Y. Zhao, H. Duan and Y. F. Song, *Angew. Chem., Int. Ed. Engl.*, 2019, **58**, 11860–11867.
- 28 G. Hu, N. Wang, D. O'Hare and J. Davis, *Chem. Commun.*, 2006, 287–289.
- 29 Y. Zhao, Q. Wang, T. Bian, H. Yu, H. Fan, C. Zhou, L. Z. Wu, C. H. Tung, D. O'Hare and T. Zhang, *Nanoscale*, 2015, **7**, 7168–7173.
- 30 J. Yu, B. R. Martin, A. Clearfield, Z. Luo and L. Sun, *Nanoscale*, 2015, **7**, 9448–9451.
- 31 J. Yu, Q. Wang, D. O'Hare and L. Sun, *Chem. Soc. Rev.*, 2017, **46**, 5950–5974.



- 32 Q. Wang and D. O'Hare, *Chem. Rev.*, 2012, **112**, 4124–4155.
- 33 Y. Wang, Y. Zhang, Z. Liu, C. Xie, S. Feng, D. Liu, M. Shao and S. Wang, *Angew. Chem., Int. Ed. Engl.*, 2017, **56**, 5867–5871.
- 34 R. Liu, Y. Wang, D. Liu, Y. Zou and S. Wang, *Adv. Mater.*, 2017, **29**, 1701546.
- 35 X. Zhang, Y. Zhao, Y. Zhao, R. Shi, G. I. N. Waterhouse and T. Zhang, *Adv. Energy Mater.*, 2019, **9**, 1900881–1900887.
- 36 Q. Wang and D. O'Hare, *Chem. Commun.*, 2013, **49**, 6301–6303.
- 37 Q. Qin, J. Wang, T. Zhou, Q. Zheng, L. Huang, Y. Zhang, P. Lu, A. Umar, B. Louis and Q. Wang, *J. Energy Chem.*, 2017, **26**, 346–353.
- 38 G. Carja, G. C. Chitanu, Y. Kameshima, H. Chiriac and K. Okada, *Appl. Clay Sci.*, 2008, **41**, 107–112.
- 39 Y. Zhao, S. He, M. Wei, D. G. Evans and X. Duan, *Chem. Commun.*, 2010, **46**, 3031–3033.
- 40 D. Kang, H. Shao, G. Chen, X. Dong and S. Qin, *Sep. Purif. Technol.*, 2021, **263**, 118371–118381.
- 41 D. Kang, H. Shao, G. Chen, X. Dong and S. Qin, *J. Membr. Sci.*, 2021, **621**, 118951–118960.
- 42 L. Li, R. Ma, Y. Ebina, N. Iyi and T. Sasaki, *Chem. Mater.*, 2005, **17**, 4386–4391.
- 43 Z. Liu, R. Ma, Y. Ebina, N. Iyi, K. Takada and T. Sasaki, *Langmuir*, 2006, **23**, 861–867.
- 44 M. Hajibeygi and M. Omid-Ghallemohamadi, *J. Polym. Res.*, 2017, **24**, 61–72.
- 45 Y. Yan, Q. Liu, J. Wang, J. Wei, Z. Gao, T. Mann, Z. Li, Y. He, M. Zhang and L. Liu, *J. Colloid Interface Sci.*, 2012, **371**, 15–19.

